COMPARISON OF CLASSICAL TOOLS AND MODERN FINITE ELEMENT MODELING IN THE ELECTRICAL DESIGN OF SLAG RESISTANCE FURNACES

Mark William Kennedy[1], Melina Garcia[2], Finn Olesen[3]

[1]Norwegian University of Science and Technology, Department of Materials Science and Engineering, N-7491 Trondheim, Norway

mark.kennedy@material.ntnu.no

[2]Elkem AS, Hoffsveien 65b, 0303 Oslo, Norway

[3]Elkem Bjølvefossen AS, Ålvikvegen 1055, 5614 Ålvik, Norway

Keywords: COMSOL, FEM, slag, resistance, furnace

Abstract

Furnace resistance is a function of the complex interrelationship between many factors including: operating practice, slag conductivity, temperature, power intensity, and geometry (electrode shape, diameter, spacing, immersion, slag depth, etc.).

Accurate prediction of resistance is critical for success of the overall furnace design. The sizing of electrodes, columns, bus-bars, and transformers are all impacted. Estimation of minimum and maximum resistance or maximum operational current, as well as the maximum operating voltage are of fundamental importance.

Various mathematical tools have been developed to assist designers with the selection of furnace dimensions and the prediction of resistance. Elkem found the methods of Downing and Urban 1965 and Westly 1975, to be particularly useful.

In the current paper, comparisons are drawn between data from spent aluminum pot lining (SPL) demonstration testing at Elkem Bjølvefossen and predictions based on these classical tools and 3D finite element modeling (FEM) with COMSOL®.

Introduction and Electrical Background

The focus of this paper will be on the estimation of the electrical resistance of a slag furnace. This paper will be confined to alternating current (AC) furnaces operating in so-called, 'slag resistance' mode. Slag furnace dimensioning will not be discussed in detail in this paper, but will be dealt with in a separate paper [1].

In the electrical design of a slag furnace, the single most important design parameter is the estimate of the furnace resistance and as a first approximation it can be assumed to be equal to the resistance between the electrodes (i.e. excluding all electrical system losses). Heat produced in a slag resistance furnace is often referred to as 'Joule' heating and can be calculated using Ohm's law:

$$P_{phase} = I_{phase}^2 R_{phase} \quad (1)$$

$$P_{furnace} = N P_{phase} \quad (2)$$

Slag resistance furnaces are either 1-phase (not uncommon at <3 MW) or 3-phase, such that N in Equation (2) is either 1 or 3. If a 3-phase furnace is used, P_{phase} represents the power supplied by each of the 3 secondary transformer phases.

In 3-phase systems it is possible to connect the transformer phases using either 'wye' (Y) or 'delta' (Δ) connections. Sometimes 'wye' is also referred to as 'star'. Transformers used with three phase slag resistance furnaces are almost uniformly connected in delta on the secondary side of the transformer. If one wishes to compare a 'wye' calculated resistance (electrode-to-bottom) to the equivalent 'delta' (electrode-to-electrode or phase resistance) one must multiply the 'wye' resistance by three.

For 3-phase furnaces: $R_{phase} = R_{delta} = 3\ R_e = 3\ R_{wye}$ (3)

The electrode current measuring transformers and voltage contacts of slag furnaces are wired as a 'wye', relative to an artificial electrical centre point on the furnace bottom. 'Wye' is selected for process control purposes, to allow the power of each electrode to be independently regulated by the electrode-bottom voltage measurement using mechanical hoist position.

Estimation of Furnace Resistance

Furnace Geometric Constants and Slag Conductivity

The resistance of a conductor depends on the area of conduction, the length of the current path and the electrical conductivity as described by Equation (4). This simplified rule applies also to the slag inside of an electric furnace.

$$R_{phase} = \frac{l}{a}\frac{1}{\sigma} \quad (4)$$

Equation (4) is deceptively simple; in the case of a slag furnace, how does one define either the length (l) or the area (a) of the conduction path or the geometric constant, ($\frac{l}{a}$)? Figure 1 gives

an indication of the complex current paths taken between any two of the electrodes, including the effect of a highly conductive metal or matte present in the bottom of the furnace. Jiao *et al.* have made a very thorough experimental and analytical review of furnace geometric constants [2-3].

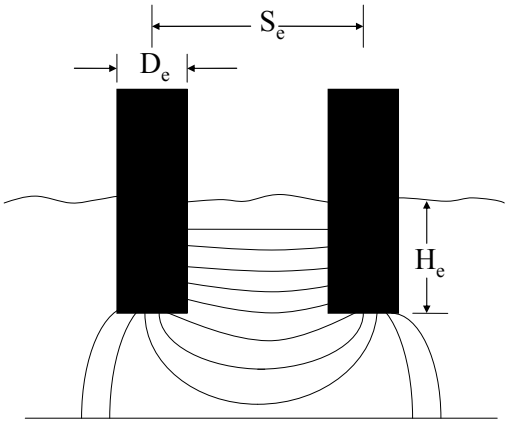

Figure 1. Electrode 'unit-cell' for evaluation of 'geometric' constants and resistance.

Typical electrical conductivity values for high silica smelting slags, are on the order of 20-30 $(\text{ohm m})^{-1}$ at 1400°C [4], while the conductivity of matte or metal are orders of magnitude higher.

Real furnace slags are typically composed of many components and it is extremely difficult to find or estimate their conductivity. Jiao *et al.* reviewed much of the available slag conductivity data and proposed useful correlations to estimate values for complex slag systems [5]. One excellent source of laboratory conductivity data for different slag systems, at a variety of temperatures, is the Slag Atlas [6]. Caution should be exercised in using laboratory conductivity data collected at kHz frequencies, to design slag furnaces operating at 0, 50 or 60 Hz. The impact of frequency on effective slag conductivity at high current (density), has not been clearly established [7].

Empirical Furnace Resistance Models

One of the first models for the scaling of furnace resistance, was that of Andreæ in 1933 [8]. Andreæ observed that furnace resistance for similar furnace charges, varied inversely with the diameter of the electrodes, as shown in Equation (5). The units of Andreæ's '*k*' are those of resistivity, [ohm m].

$$k = \frac{V_{electrode}}{I_{electrode}} \pi D_e \tag{5}$$

In accordance with Andræe's concept, when designing an efficient slag furnace, the smallest reasonable electrode diameter should be selected, along with the number and type. Excessively large electrodes will reduce the furnace resistance, increasing current, transformer, bus, and hoist size, reducing the power factor and so on. Interaction between the electrical design and the furnace dimensioning, may force the selection of larger diameter or better quality electrodes, greater number, and alternate furnace shape to accommodate them. These issues are outside of the scope of the current paper.

Kelly [9] and later Persson [10] examined the variation of '*k*' values with changing furnace conditions, i.e. furnace power intensity and hence slag temperature for different processes. These methods proved very useful for the scaling of both slag containing furnaces and arc furnaces.

Many design tools originally intended for use with submerged arc furnaces, have proven useful when applied to slag processes. The method of Downing and Urban [11] has been used with some success for example by Elkem. This model is based on the electric field and capacitance produced by an infinitely long charged conductor and a sphere in an infinite medium. The derivation of the requisite equations can be found in the book by Attwood [12]. Persson [13] subsequently modified the equation to allow for flat and intermediate shaped electrode tips. The resulting equation is given as Equation (6), in resistance form. The first term represents the contribution of the cylindrical part of the electrode and the second that of the tip. The original equation was derived by means of successive imaging. The current authors have replaced the 'series' expansion in the second term, to make the equation both shorter and more accurate than the original truncated version, presented by Downing and Urban.

$$R_{phase} = \frac{1}{\sigma}\left\{ \frac{\pi H_e}{\ln\left(\frac{S_e}{2r_e} + \sqrt{\left(\frac{S_e}{2r_e}\right)^2 - 1} \right)} + a r_e \left(\frac{1}{1 - \frac{r_e}{S_e}} \right) \right\}^{-1} \tag{6}$$

Where: R_{phase} is the 'delta' resistance between 2 electrodes [ohms], σ is the 'representative' or 'effective' slag conductivity [S/m], H_e is the electrode immersion measured from the tip [m], a is the tip parameter [dimensionless], r_e is the effective electrode radius for the immersed portion of the electrodes [m], and S_e is the electrode spacing measured centre-to-centre [m]. The 'tip' parameter 'a' in Equation (6) is π for a hemispherical tip, as per Downing and Urban's original equation or 2 for a flat tip as proposed by Persson. Persson also proposed 2.5, as an 'intermediate' value and this was adopted by Elkem as a standard reference value for a worn electrode. Elkem has also adopted a standard 60% factor for the effective radius of the immersed section of the electrode also to account for wear. If the tip can be examined, it is possible to derive geometrically both the average worn diameter and an approximate value for the tip parameter 'a' based on the radius of curvature of the tip of the electrode and the effective electrode radius using Equation (7). An infinite radius of curvature is effectively a flat tip.

$$a = \pi - (\pi - 2)\left(\frac{r_{tip} - r_e}{r_{tip}} \right) \tag{7}$$

A dip measurement can be performed on a real lab, pilot, demonstration or commercial scale furnace, to estimate the conductivity by using Equations (6) and (7). Elkem performed a dip test in a 600 kW furnace using 35 cm diameter, high quality graphite electrodes. The effective electrode diameter was 78% of the original and tip parameter was determined from physical measurements to be 2.86 using Equation (7). The slag was of a known composition and temperature. The measured conductivity was 0.6 $(\text{ohm cm})^{-1}$, which compared well with the literature estimate of 0.66 $(\text{ohm cm})^{-1}$.

Definition of the 'Downing Region'

The 'Downing' region has been observed by experience to lie approximately between 20% and 80% electrode immersion (measured as a percentage of the total slag depth). When the electrodes just touch the surface of a slag bath, the furnace typically operates in 'brush arc' mode if there is sufficient voltage applied. The Downing and Urban equation applies after the arc is extinguished and until the electrode tips approach close enough to the bottom, such that the zone of high voltage gradient intercepts the highly conductive bottom. At this point the resistance begins to fall rapidly with further immersion. An example of a dip measurement, covering the full range of electrode immersions starting from brush arc, is available in the literature [14].

Practical Application of the Downing and Urban Equation (6) and Comparison with FEM

Elkem piloted the spent aluminum pot lining (SPL) smelting process in 1993 using a 600 kW, two graphite electrode, single phase furnace [15]. This process uses the carbon component of the SPL to reduce iron oxide to produce pig iron and stabilizes the fluoride in a highly acidic and chemically stable, non-leaching silicate slag. A typical assay of SPL slag is given in Table I from both the pilot and demonstration testing.

The high silica, alumina, sodium and fluoride containing slag produced by this process, was unique and thus there was no literature or industrial benchmark conductivity information available. A series of dip tests were, therefore, conducted during the original piloting to estimate the slag conductivity using Equation (6).

Table I. SPL Slag Data from Pilot Plant and Demonstration Plant Dip Tests

Slag Component	Pilot (wt%)	Demonstration (wt%)
F	5.9	7.0
FeO	8.7	8.1
SiO_2	43.0	44.7
CaO	3.3	5.9
Na_2O	19.3	13.9
Al_2O_3	17.2	21.7
K_2O	0.3	1.6
MgO	1.3	1.2
Slag conductivity, $(ohm\ cm)^{-1}$	154	32
Temperature, ^oC	1377	1390

For the composition and temperature shown in Table I, the slag was found to have a representative conductivity of 154 $(ohm\ m)^{-1}$, as shown in Figure 2 over the 'Downing region', for two pilot dip tests. Also shown on Figure 2 are the results of the 3D COMSOL® FEM model, which over the same region, averages 134 $(ohm\ m)^{-1}$. The deviation between the models is only 15%, and well within acceptable limits for design purposes. The degree of agreement between Equation (6) and FEM seen in Figure 2 is typical.

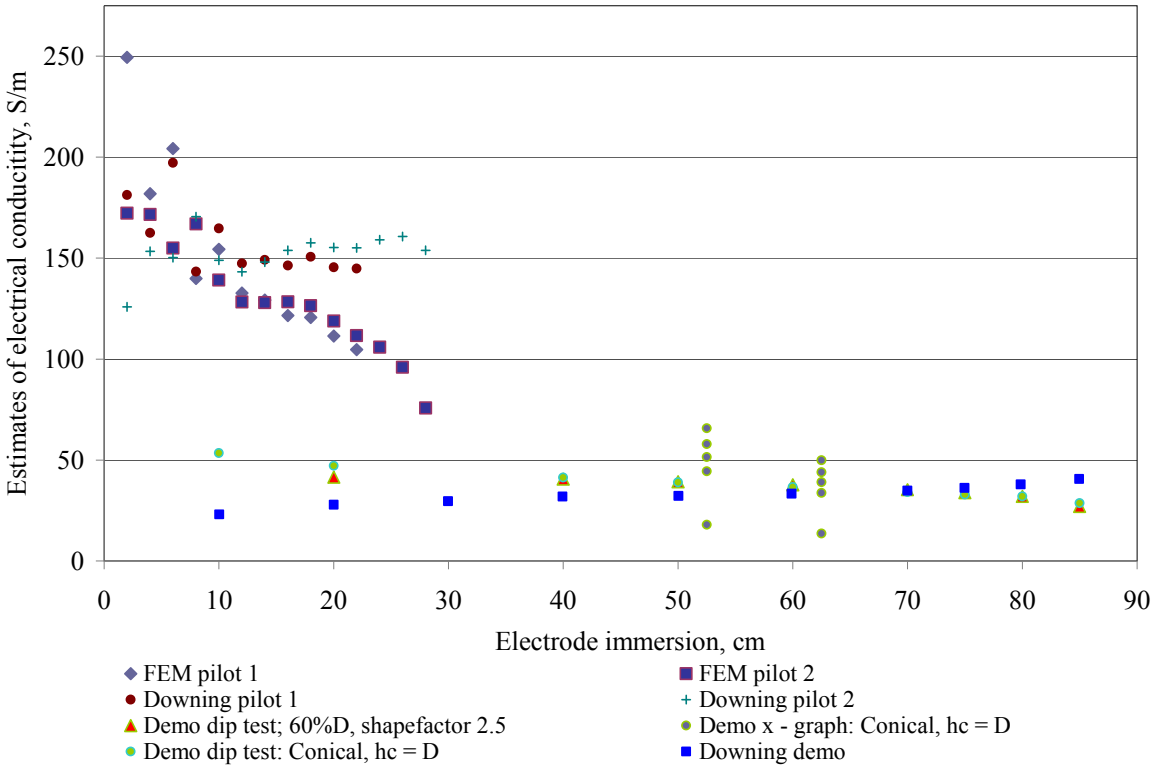

Figure 2. Comparison between electrical conductivities estimated using Equation (6) and 3D COMSOL® FEM for the SPL pilot and demonstration dip tests.

The SPL smelting process was recently demonstrated at Elkem Bjølvefossen, on an existing industrial 18 MVA, 6 m diameter furnace (measured at the inside of the refractory). This furnace used 950 mm Søderberg electrodes, spaced 2.35 m apart. Dip tests were performed on the demonstration furnace on a number of occasions. The data shown in Table I were collected on a day of operation at 10 MW (354 kW/m^2 of projected hearth area). The results from the demonstration dip test are also plotted in Figure 2.

A representative photo of the actual Søderberg electrodes in use, a 'realistic' electrode sketch and the Elkem 'standard' worn electrode shape, are all shown in Figure 3. Both the 'realistic' and 'standard' shapes were used during FEM modeling. The agreement between the FEM and Downing estimates using the 'standard' shaped electrodes was good for the demonstration test, with a difference of only 18%. A good study of the impact of electrode shape, immersion and furnace dimensions on resistance, can be found in the literature [16].

The following observations can be made from the data presented in Table I and Figure 2:

1. The Downing and FEM results are in good agreement, both for the pilot and demonstration plants using the 'standard' shaped electrodes.
2. FEM results obtained from the 'realistic' shaped electrodes are not significantly different than with the 'standard' shaped electrodes, for the demonstration plant dip test.
3. The slag electrical conductivity was not the same for the pilot and demonstration plants!
4. A scale up based on the pilot plant results (either Downing or FEM) would have resulted in a sub-optimal transformer specification.

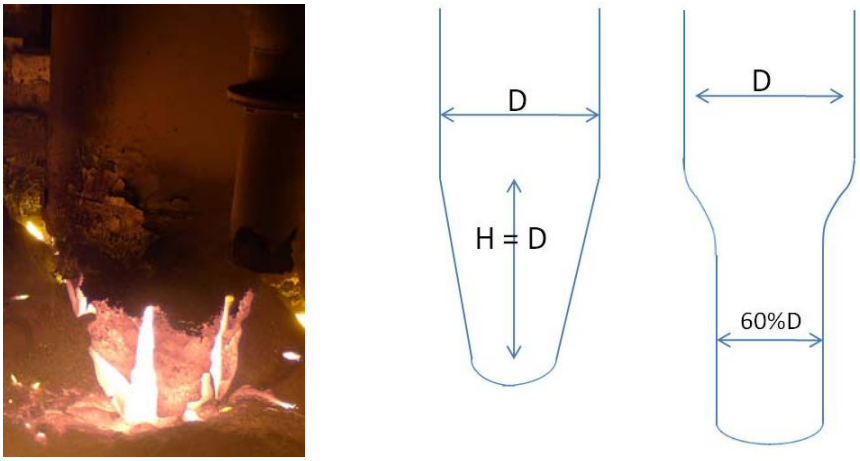

Figure 3. Picture of the tip of a typical Søderberg electrode and shapes used for FEM modeling, 'Realistic' and Elkem 'Standard'.

The demonstration test at Bjølvefossen utilized existing equipment, which had adequate transformer voltage range to compensate for the surprisingly low slag conductivity. The cause for the change in apparent slag conductivity has not been clearly identified. It could be due to electronic rather than ionic transport of current during the pilot campaign, either through the charge or via the Fe^{2+}/Fe^{3+} in the slag phase, as shown in some recent publications [17-19]. Speciation of the slag phase iron by valance, for example using Mössbauer spectroscopy is recommended to study such effects. SPL and iron oxides fed to the pilot plant in 1993, were not identical to those fed in 2008/9, which may also have been a factor.

The dramatic shift in apparent slag conductivity should be a warning of the risks involved and care required in the scale up of new slag furnace processes. This risk is magnified by poor understanding of the real modes of conduction in such systems and the corresponding dependence on over simplified electrical models (both semi-analytical/empirical and FEM).

Due to the very long delivery time of furnace transformers, the power supplies specified for new processes must be designed with more flexibility both in terms of voltage and current ranges, making them less 'optimized' and more expensive to purchase. The configuration of secondary transformer coils can be designed such that there is increased flexibility in the voltage and current (i.e. reconfiguring secondary coils from parallel to series connections).

Relationship between Resistance, Power Intensity and Temperature

Two main relationships are necessary to predict the operating resistance of a slag furnace:

1. Variation of resistance due to changes in geometry (Downing and Urban, Equation (6) or FEM analysis), and
2. Effect of power intensity on operating resistance.

The relationship between power intensity and changes in furnace temperature and hence resistance is complex, and can't yet be predicted based on fundamentals. This relation is affected by the size, temperature, density and composition of the feed, the fraction of the energy used for chemical reduction, the operation of the furnace (open bath or feed covered), electrode tip position (deep or shallow), furnace construction (insulated roof or open top), etc.

Westly [20-21] studied the operation of many different arc furnace processes and by regression and dimensional analysis found a correlation between furnace current and power intensity:

$$I_e = C_3 * P_{furnace}^{X} \quad (8)$$

Where the exponent X is ~0.67 for most arc furnace processes. Equation (8) implies that resistance decreases with higher power intensity, which is a reasonable assumption for both arc and slag furnaces. The relation between X, voltage and resistance can be derived from Ohm's law:

$$V_e = C_1 * P_{furnace}^{(1-X)} \quad (9)$$
$$R_e = C_2 * P_{furnace}^{(1-2X)} \quad (10)$$

Using Equation (10), the impact furnace power intensity has on resistance can be estimated, without direct knowledge of the slag temperature or measurement of slag properties as a function of temperature. In-furnace temperature data is typically not available for slag furnaces, due to the high operating temperatures and the corrosive action of the slag.

X must fall between 0.5 (constant resistance) and 1.0 (constant voltage). High X values indicate either that the slag gets much hotter for each incremental increase in power or that the slag conductivity increases very quickly with temperature. For ferronickel furnaces, X has been found to vary from 0.65 to 0.80 [22]. A value of X=0.78 has been estimated for the SPL process by regression of the furnace current against power, with an R^2 of 0.91.

The same furnace operating data used in the X-graph analysis, at power intensities from 4 to 10 MW, have been analyzed using the 3D FEM model and the range of slag conductivity estimated. Values are plotted in Figure 2, for different assumed depths of electrode immersion.

Conclusions

Acceptable agreement is found between the FEM solutions using a 3D COMSOL® model and the Downing and Urban Equation (6). Westly's formulae provide a convenient method of adjusting predicted resistance for changes in the furnace operating power intensity. Measurement of slag properties with one set of feed, at one scale, is no guarantee of a successful scale up with slightly altered feed, in a much larger dimensioned furnace. Lack of understanding of conduction and impedance in slags (e.g. electronic vs. ionic conductivity), limit our ability to generate robust electrical models and to design optimized furnace power supplies.

Acknowledgements

The permission of Elkem Bjølvefossen to publish results from the SPL pilot and demonstration scale testing is gratefully acknowledged.

References

1. M. W. Kennedy, "Electric Slag Furnace Dimensioning Criteria," Submitted to the *International Smelting Technology Symposium (Incorporating the 6th Advances in Sulfide Smelting Symposium), TMS*, Orlando Florida, (2012).
2. Q. Jiao, "Generation and Transmission of Heat in an Electric Slag Resistance Furnace," *Dissertation Abstracts International (USA),* 52, (1992), 222.
3. Q. Jiao and N. Themelis, "Correlation of Geometric Factor for Slag Resistance Electric Furnaces," *Metallurgical and Materials Transactions B,* 22, (1991), 183-192.
4. R. Eric, "Slag Properties and Design Issues Pertinent to Matte Smelting Electric Furnaces," *Journal of the South African Institute of Mining and Metallurgy,* 104, (2004), 499-510.
5. Q. Jiao and N. Themelis, "Correlations of Electrical Conductivity to Slag Composition and Temperature," *Metallurgical and Materials Transactions B,* 19, (1988), 133-140.
6. K. Mills, "Slag Atlas," *VDEh 2nd Edition, Verlag Stahleisen GmbH, Düsseldorf,* (1995)
7. K. Mills, "The Estimation of Slag Properties, a Short Course," *Southern African Pyrometallurgy 2011*, (2011), 1-56.
8. F. Andreae, "Design and Control of Ferroalloy Furnaces," *Transactions of the American Institute of Electrical Engineers,* 69, (1950), 557-562.
9. W. Kelly, "Design and Construction of the Submerged Arc Furnace," *Carbon and Graphite News, Vol. 5, No.* 1, (1958).
10. J. Persson, "The Significance of Electrode-to-Hearth Voltage in Electric Smelting Furnaces," *Electric Furnace Conference*, (1970), 168-169.
11. J. Downing and L. Urban, "Electrical Conduction in Submerged Arc Furnaces," *Journal of Metals,* 18, (1966), 337-344.
12. S. S. Attwood, *Electric and Magnetic Fields* (New York: Dover, 1967).
13. J. Persson, "Conduction Characteristics of Electric Furnaces," in *Electric Furnace Conference*, (1978), 168-169.
14. B. Boulet, V. Vaculik, and G. Wong, "Control of Non-Ferrous Electric Arc Furnaces," *IEEE Canadian Review,* (1997), 1-13.
15. E. Q. Dahl, "The Elkem Process for Treatment of Spent Potlining," *Light Metals 1996*, Montreal, Canada, (1996), 99-105.
16. A. Jardy, D. Ablitzer, and S. Jorget, "Modelling of Slag Behaviour in a Non-Ferrous Smelting Electric Furnace," *The Reinhardt Schuhmann International Symposium on Innovative Technology and Reactor Design in Extraction Metallurgy*, (1986), 419-431.
17. A. Ducret, D. Khetpal, and D. R. Sadoway, "Electrical Conductivity and Transference Number Measurements of FeO-CaO-MgO-SiO_2 Melts," Presented at Electrochemical Society Meeting, Philadelphia, May 2002, (2002), 347-53.
18. M. Barati and K. S. Coley, "Electrical and Electronic Conductivity of CaO-SiO_2-FeO_x Slags at Various Oxygen Potentials: Part I. Experimental Results," *Metallurgical and Materials Transactions B,* 37, (2006), 41-49.
19. M. Barati and K. S. Coley, "Electrical and Electronic Conductivity of CaO-SiO_2-FeO_x Slags at Various Oxygen Potentials: Part II. Mechanism and a Model of Electronic Conduction," *Metallurgical and Materials Transactions B,* 37, (2006), 51-60.
20. J. Westly, "Critical Parameters in Design and Operation of the Submerged Arc Furnace," in *Electric Furnace Conference*, (1975), 47-53.
21. J. Westly, "Resistance and Heat Distribution in a Submerged-Arc Furnace," *Proceedings of INFACON 74 Johannesburg*, (1975), 121-127.
22. A. A. Dor, H. Skretting, and C. M. Engineer, "The Production of Ferro Nickel by the Rotary Kiln-Electric Furnace Process," *International Laterite Symposium*, (1979), 459-490.